Biosensors and Bioelectronics 64 (2015) 36–42

Contents lists available at ScienceDirect

Biosensors and Bioelectronics

journal homepage: www.elsevier.com/locate/bios

Quartz crystal microbalance with dissipation and microscale thermophoresis as tools for investigation of protein complex formation between thymidylate synthesis cycle enzymes

Anna Antosiewicz*, Elżbieta Senkara, Joanna Cieśla

Institute of Biotechnology, Faculty of Chemistry, Warsaw University of Technology, Noakowskiego 3, 00-664 Warsaw, Poland

ARTICLE INFO

Article history:
Received 9 May 2014
Received in revised form
11 August 2014
Accepted 18 August 2014
Available online 22 August 2014

Keywords:
Quartz crystal microbalance
Microscale thermophoresis
Protein complex
Thymidylate synthase
Dihydrofolate reductase
Thymidylate biosynthesis

ABSTRACT

Thymidylate synthase (TS) and dihydrofolate reductase (DHFR) play essential role in DNA synthesis, repair and cell division by catalyzing two subsequent reactions in thymidylate biosynthesis cycle. The lack of either enzyme leads to thymineless death of the cell, therefore inhibition of the enzyme activity is a common and successful tool in cancer chemotherapy and treatment of other diseases. However, the detailed mechanism of thymidylate synthesis cycle, especially the interactions between cycle enzymes and its role remain unknown.

In this paper we are the first to show that human TS and DHFR enzymes form a strong complex which might be essential for DNA synthesis. Using two unique biosensor techniques, both highly sensitive to biomolecular interactions, namely quartz crystal microbalance with dissipation monitoring (QCM-D) and microscale thermophoresis (MST) we have been able to determine DHFR–TS binding kinetic parameters such as the K_d value being below 10 μM (both methods), $k_{on}=0.46\times10^4\ M^{-1}\ s^{-1}$ and $k_{off}=0.024\ s^{-1}$ (QCM-D). We also calculated Gibbs free energy as in the order of −30 kJ/mol and DHFR/TS molar ratio pointing to binding of 6 DHFR monomers per 1 TS dimer (both methods). Moreover, our data from MST analysis have pointed to positive binding cooperativity in TS–DHFR complex formation. The results obtained with both methods are comparable and complementary.

1. Introduction

Thymidylate synthase (TS, EC 2.1.1.45), dihydrofolate reductase (DHFR, EC 1.5.1.3) and serine hydroxymethyltransferase (SHMT, EC 2.1.2.1) are enzymes constituting the thymidylate biosynthesis cycle and providing *de novo* synthesized thymidylate that is crucial for DNA synthesis and repair (Carreras and Santi, 1995; Liu et al., 2002; Kisliuk, 2006). Previous studies have shown that lack of TS and DHFR enzymes or inhibition of their activity leads to the thymineless death of a cell, as DNA cannot be synthesized due to the deficiency of thymidylate derivative - deoxythymidine triphosphate (dTTP). Therefore, the enzymes are highly important drug targets in many different disorders including cancer (Wilson et al., 2014).

In most organisms, including human, these enzymes function as distinct proteins, however in protozoa and plants they are encoded by a single gene and expressed as a bifunctional enzyme DHFR-TS with autonomous binding sites, similar to those of monofunctional enzymes. Taking this under consideration, we have suspected that human monofunctional TS and DHFR form an active complex while involved in thymidylate synthesis cycle.

Years of meticulous studies devoted to this cycle highlight its importance and have indicated the possibility that the protein–protein interactions and formation of metabolic complex may be necessary for cells to proliferate. McGaughey et al. (1996), using affinity chromatography, have demonstrated the specific binding between immobilized T4 bacteriophage-encoded dCMP deaminase (the enzyme providing dUMP for TS reaction) and TS, as well as DHFR and several other proteins involved in DNA metabolism and repair. The results obtained by Reddy and Pardee (1980) on mammalian cells were supporting the hypothesis that six enzymes involved in DNA metabolism (TS and DHFR among them) were translocated into nuclei of cells that are about to replicate DNA, and form the complex that was named by the authors “replitase”. The authors suggested that the assembly of the complex possibly signaled the initiation of the S phase of the cell cycle. Finally, recent studies presented by Stover group have shown that in mammalian cells SHMT serves as a scaffold protein translocating

* Corresponding author. Tel.: +48 22 234 75 07; fax: +48 22 628 27 41.
E-mail addresses: aantosiewicz@ch.pw.edu.pl (A. Antosiewicz), esenkara@ch.pw.edu.pl (E. Senkara), jciesla@ch.pw.edu.pl (J. Cieśla).

http://dx.doi.org/10.1016/j.bios.2014.08.031
0956-5663/

DHFR and TS to nucleus to assemble the complex required for DNA replication and repair. This translocation was essential to prevent uracil accumulation in nuclear DNA. Moreover, nuclear *de novo* thymidylate synthesis appeared to be critical for maintaining DNA integrity (Anderson et al., 2012; MacFarlane et al., 2011; Woeller et al., 2007). However, in spite of some evidence supporting formation of the complex between TS and DHFR, the detailed mechanism of thymidylate synthesis cycle functioning, especially the nature of protein–protein interactions between particular enzymes remains unknown.

The aim of our studies is to prove the existence of such interactions and fully analyze the human TS–DHFR complex formation, as it most likely is necessary for the DNA synthesis to occur. The obtained data might be of great importance especially in anticancer drug development, where the rising problem is the increase of target enzyme resistance to inhibitor (Banerjee et al., 2002; Volpato and Pelletier, 2009). The elucidation of interactions between thymidylate synthesis cycle enzymes may lead to development of such new category of drugs that could target the DHFR–TS complex formation (instead of either enzyme catalytic activity) and, consequently, cause inhibition of DNA synthesis.

In this paper we present evidence for *in vitro* human DHFR–TS complex formation using unique biomolecular interaction analysis tools. The protein–protein binding has been detected and characterized with the use of two sensitive techniques: quartz crystal microbalance with dissipation monitoring (QCM-D) and microscale thermophoresis (MST).

Quartz crystal microbalance is a thickness shear mode acoustic wave resonator that has become widely popular for studying various biological processes due to its satisfactory performance (Cooper and Singleton, 2007). In this method mass uptake on sensor's surface can be registered as changes of quartz crystal oscillator resonance frequency due to piezoelectric phenomenon (Okahata et al., 2000; Tan et al., 2009). The main advantages of this method include high sensitivity, rapid and facile operation and label-free monitoring (Tan et al., 2009). In this work, a QCM-D was used as a tool not only to detect biomolecular recognition in aqueous solution but also to characterize the binding kinetics of the studied interactions. The viscoelastic layers of water rich protein adsorbents have been characterized using the dissipation mode which allows for monitoring of the energy damping due to frictional movement and conformational changes of the molecules immobilized on the quartz oscillator (Limson et al., 2004; Nicolini et al., 2012).

One of the most common application areas of QCM-D includes the investigation of protein–protein interactions (Cooper and Singleton, 2007; Spera et al., 2013). This technique enables determination of analyzed interactions specificity, kinetics and proteins affinities. Moreover, it is also possible to evaluate the kinetic profile of protein adsorption and associated conformational change on various surfaces (Shen et al., 2001). There have also been reports on using QCM-D for the investigation of adsorption/desorption cycles (Si et al., 2002), protein subunits and peptides screening (Melles et al., 2005), density analysis of proteins (Voros, 2004) as well as solvent and ions influence on protein–protein interactions (Sadik and Cheung, 2001).

Microscale thermophoresis is a free solution technique used for biomolecular interactions studies, that can be carried out in wide range of buffers and biological liquids (Duhr and Braun, 2006; Wienken et al., 2010). It allows a quantitative analysis of protein interactions by exploiting a unique phenomenon of thermo diffusion describing the variable movement of different particles along temperature gradient. The movement of molecules in the generated heat-wave differs according to various molecular properties and additionally further diverge while binding to the second particle. Therefore, unlike the most of biophysical techniques, MST is highly sensitive to alterations of wide variety of molecule parameters occurring during complex formations, from changes in particle mass and charge to modifications in molecule conformation and hydration shell (Seidel et al., 2013). Moreover, as a technique conducted in buffer solution, it enables *in vitro* studies on molecules binding without the need of immobilizing one of the particles, regardless of binding partner size or physical properties.

The MST technique is a highly adequate method for protein–protein interactions studies, since it enables monitoring of the protein complex formation, gives an insight into mechanism of binding and allows determination of the process kinetics. MST can be utilized as a tool for evaluation of protein complexes dissociation coefficient in experiments involving either incubation of purified recombinant proteins (Hallström et al., 2013; Latz et al., 2013), additional incubation of proteins with their cofactors (Jerabek-Willemsen et al., 2011), or cell lysate probed with protein in search of the binding partner (Derler et al., 2013). The method allows for monitoring of the formation of protein dimers, tetramers and higher oligomer structures (Liu et al., 2013). In addition, MST enables measurements of the antibody affinity towards target protein as well as affinity changes upon protein modifications that further lead to elucidation of the exact epitope recognized by a given antibody (Miles et al., 2013).

In this work we combine these two ultra-sensitive and novel techniques as tools for characterizing the protein–protein interactions of the enzymes involved in thymidylate synthesis cycle. To our knowledge, to date there are no reports on complying these two methods together which is a new approach in characterizing the protein–protein complex formation. We show that these tools are complementary for biomolecular analysis and allow characterization of the kinetic parameters of the complex formation.

2. Materials and methods

2.1. Enzymes preparation

Methods for preparation of the recombinant human thymidylate biosynthesis cycle enzymes, as well as the source of recombinant human CK2α protein and lipase Amano AY30 utilized in this paper studies are to be found in Supporting information, Appendices A.

2.2. Quartz crystal microbalance with dissipation monitoring (QCM-D) measurements

QCM-D measurements were carried out using commercially available HisTag capturing sensors (5 MHz, QSX 340, Q-Sense) that consist of chelated Cu^{2+} ions coupled to a passivating PEG background coating. Prior to the experiments the sensor's surface was cleaned according to the manufacturer protocol. The frequency and dissipation variations were monitored using Q-Sense E1 QCM-D (Q-Sense, Sweden) device equipped with a liquid flow cell setup. All experiments were carried out in the following protein buffer solution: 20 mM Tris–HCl (pH 7.6) containing 100 mM NaCl, 10 mM $MgCl_2$ and 0.05% Tween 20 at 200 μl/min flow rate and 25 °C.

2.2.1. In-situ quartz crystal functionalization with HisTag labeled TS

In a typical QCM-D experiment, the receptor molecules are immobilized on the surface of the quartz crystal, while the ligand molecules are freely dissolved in the surrounding solution. In the present work, TS with HisTag label served as a receptor, therefore it was immobilized on the surface of the sensor according to the following procedure.

A clean quartz crystal sensor was mounted in the measuring chamber with the liquid flow cell setup. The background signal was established on protein buffer solution (20 mM Tris–HCl pH 7.6 containing 100 mM NaCl, 10 mM $MgCl_2$ and 0.05% Tween 20) at 200 μl/min flow rate to obtain stable Δf and ΔD baseline signals. In order to immobilize the protein on the surface of the sensor, 1 ml volume of 0.25 μM TS with HisTag label was introduced into the system in a closed circulating continuous 200 μl/min flow rate for 30 min. The changes of Δf and ΔD values due to protein adsorption on the surface were recorded in real time. For each experiment we have obtained Δf values in the range of -30 ± 3 Hz which gives 90% reproducibility and ΔD values of $(0.230 \pm 0.016) \times 10^{-6}$ with 93% reproducibility. Finally, the whole system was washed for 10 min with protein buffer solution in order to remove any not specifically bound molecules. Data showing mass change *versus* time during TS immobilization is supplemented in Supporting information, Appendices B (Fig. B.1).

2.2.2. QCM-D control measurements

In order to rule out any unspecific binding of DHFR to the surface of the sensor, measurements with HisTag free and HisTag labeled DHFR were conducted. The procedure was done according to the protocol described in Section 2.2.1 but instead of TS, labeled or not labeled DHFR was used. Real-time curves obtained during experiments showed no frequency or dissipation change for HisTag free DHFR, in contrast to HisTag labeled enzyme (mass change *versus* time is showed in Supporting information, Appendices B (Fig. B.2)). This indicates that DHFR without HisTag label does not interact with the surface itself, therefore might be used for investigating TS–DHFR interactions on TS-modified crystal sensor.

2.2.3. QCM-D protein–protein assay

TS–DHFR complex formation experiments involved three steps performed after TS quartz crystal functionalization: (A) protein buffer solution flowing to stabilize the signals; (B) introduction of 1 ml DHFR (concentration varied from 1 to 6 μM) in closed continuous flow for 30 min; (C) rinsing with protein buffer solution to remove excess unbound molecules.

The reported data were modeled and analyzed using the Sauerbrey model, viscoelastic Voigt model and kinetic models (Hook and Kasemo, 2001) with use of the QSense and QTools data analysis software (Q-Sense, Sweden). Exemplary measurement of mass change *versus* time obtained during QCM-D protein–protein assay is given in Supporting information, Appendices B (Fig. B.3). The experiments were repeated at least three times for each measurement. The reported mass change is an arithmetical average of the experiments; the reported errors are calculated as standard deviation.

2.3. Microscale thermophoresis (MST) measurements

Microscale thermophoresis allows studying biomolecular interactions in a solution by measuring the mobility of molecules exposed to microscopic gradients of temperature generated by an IR-Laser. Upon interacting with the binding partner, the movement of the fluorescently labeled receptor molecule is altered; the mobility changes are detected and plotted to obtain the protein binding curves.

In quantification of the binding in molecules interaction, MST exploits fluorescence (F) response of the labeled molecule which corresponds to Soret coefficient (Jerabek-Willemsen et al., 2011; Seidel et al., 2013):

$$F_{\mathrm{Norm}} = F - F_0 \quad (1)$$

$$F_{\mathrm{Norm}} = 1 + \Delta T(\Delta F/\Delta T - S) \quad (2)$$

where F_{Norm} is the normalized fluorescence and F_0 is the initial fluorescence value. Soret coefficient (S) value is described by $S = D_T/D$, where D_T is constant thermal diffusion coefficient and D is a diffusion coefficient.

2.3.1. MST buffer optimalization

Bearing in mind the most preferable conditions for probe proteins, the most suitable buffer for MST experiments was chosen from the Tris buffer solutions which were fairly similar to the enzymes' storage buffer. We have verified the following variants: 20 mM and 50 mM Tris–HCl buffers (pH: 7.6; 7.8 or 8.0) containing 100 mM NaCl and with or without: 10 mM $MgCl_2$, 0.05% Tween-20, 10 mM 2-mercaptoethanol, 40% glycerol. Finally 20 mM Tris–HCl buffer pH 7.6 containing 100 mM NaCl, 10 mM $MgCl_2$, 40% glycerol and 0.05% Tween 20 was selected and used in all experiments. The chosen buffer was adequate for stabilization of the studied enzymes and did not show any background fluorescence under conditions employed in the study.

2.3.2. Capillary selection

Prior to the experiments, initial capillary scans were performed. The fluorescence levels of the labeled TS protein were measured using the following types of glass capillaries suitable for the MST Monolith NT device: standard treated capillaries, hydrophobic capillaries, hydrophilic capillaries, and enhanced gradient capillaries (standard treated, hydrophobic and hydrophilic). Taking into account the scanning results, hydrophobic capillaries were chosen for all the experiments.

2.3.3. MST protein–protein interactions evaluation

MST measurements were conducted using Monolith NT.115 instrument (NanoTemper Technologies, Germany). Thymidylate synthase and serine hydroxymethyltransferase (SHMT) were fluorescently labeled with L001 Monolith NT.115 Protein Labeling Kit RED-NHS (Amine Reactive) dye according to manufacturer protocol. Unlabeled studied proteins did not show any intrinsic fluorescence. Increasing concentrations of unlabeled DHFR (5.54 nM–181.5 μM), CK2α (0.58 nM–19.1 μM) or lipase Amano AY30 (1 nM–32 μM) were titrated against 0.3 μM labeled TS. Additionally, unlabeled TS (1.9 nM–62 μM) was titrated against labeled SHMT (0.2 μM). The mixtures were incubated at room temperature and centrifuged for 5 min at 16,100*g* to remove any potential aggregates. The supernatants were soaked into capillaries and transferred to the MST instrument. Assays were conducted at 40% and 80% of IR-laser power.

2.4. Analysis of protein–protein binding molar ratio

The stoichiometry of TS–DHFR binding studied by means of QCM-D was estimated from Scatchard equation. The concentration of the ligand bound was calculated from the amount of mass increase due to the complex formation on TS-modified sensor. The concentration of the free ligand was calculated from the difference between the total concentration of ligand and the concentration of ligand bound. The total receptor concentration was calculated by modeling the data obtained during the immobilization of TS protein on a QCM-D sensor.

The molar ratio of complex partners was also calculated using the data obtained by means of MST. In this case binding characteristics of protein–protein interaction was analyzed as described in Möller and Denicola (2002). A linear relationship between fluorescence intensity (F) and concentration of unlabeled protein (P_t) was delineated, allowing calculation of the molecules concentration bound to TS (P_b): $P_b = (F - F^0)/\alpha$, where F^0 is the fluorescence of the unbound TS and α is a proportionality coefficient of the $F = f(P)$ function. Concentration of free unlabeled

protein (P_f) was calculated from the difference: $P_f = P_t - P_b$. Stoichiometry of the interaction was calculated from the plateau of MST curve highly above the obtained K_d value.

3. Results and discussion

3.1. QCM-D-based studies of DHFR–TS complex formation

The Langmuir equation (Eq. (3)) describes the coverage of the molecules adsorbed on a solid surface (Ebara and Okahata, 1994; Pei et al., 2005), where Δm and Δm_{max} are the mass change and mass change upon saturation, respectively.

$$\Delta m = \frac{\Delta m_{max} K_a [\mathrm{DHFR}]}{1 + K_a [\mathrm{DHFR}]} \quad (3)$$

By plotting the mass shifts as a function of ligand concentration (Fig. 1A) the following Langmuir type adsorption isotherm was fitted to the experimental data and therefore, the equilibrium association ($K_a = 0.13 \pm 0.01\ \mu M^{-1}$) and dissociation ($K_d = 7.6 \pm 0.7\ \mu M$) constants were obtained.

The equilibrium dissociation and association constants can be additionally described by the association (k_{on}) and dissociation (k_{off}) rate constants which are correlated to the binding and unbinding of the molecules (Eq. (4)). If the protein binding does not significantly change the viscoelastic properties of the adsorbed layer, it is possible to determine k_{on} and k_{off} using the relaxation rate constant τ^{-1} which is the function of resonance frequency change (Eq. (5)).

$$\tau^{-1} = k_{on}[\mathrm{DHFR}] + k_{off} \quad (4)$$

$$\Delta f = \Delta f_{max}\left(1 - \exp\left(-\frac{t}{\tau}\right)\right) \quad (5)$$

This kinetic model was used to determine the values of τ^{-1} for each DHFR concentration and association and dissociation rate constants have been calculated (Fig. 1C). The obtained values were $k_{on} = (0.46 \pm 0.11) \times 10^4\ M^{-1}\ s^{-1}$ and $k_{off} = 0.024 \pm 0.006\ s^{-1}$, respectively.

Additionally, the Gibbs free energy for DHFR–TS binding was determined using the Van't Hoff isotherm: $\Delta G = -RT \ln(K_a)$, where R is the gas constant and T is the temperature. The obtained values were -29.19 ± 0.21 and -30.2 ± 1.3 kJ/mol calculated for Langmuir isotherm and relaxation rate constant, respectively. The molar ratio of TS and DHFR binding analyzed by the Scatchard plot (Fig. 3A) pointed to binding 6.19 ± 0.23 mol of DHFR to one mole of TS. K_d obtained from Scatchard plot was $7.5 \pm 0.6\ \mu M$.

We have also conducted several measurements of resonance frequency and dissipation change by titrating with TS the SHMT immobilized sensor. The results indicated no protein–protein binding (Supporting information, Appendices B (Fig. B.4)).

3.2. Determination of DHFR–TS binding affinities using MST analysis

The equilibrium dissociation constant (K_d) for DHFR–TS complex formation was calculated using fitting to logistic sigmoidal curve performed in Origin 6.1 program (Eq. (6)).

$$y = \frac{A_1 - A_2}{1 + (x/x_0)^p} + A_2 \quad (6)$$

where A_1 is initial F_{Norm} and A_2 is final F_{Norm}. K_d parameter is represented in the equation by x_0 value (x value in the inflexion point of the curve).

The obtained K_d value was $2.8 \pm 0.4\ \mu M$ (mean results obtained from three independent experiments ± SD). Dependence of F_{Norm} on DHFR concentration in the presence of labeled TS is given in Fig. 2A. Computation of other kinetics parameters pointed to values of $K_a = 0.37 \pm 0.06\ \mu M^{-1}$ and $\Delta G = -31.7 \pm 0.4$ kJ/mol.

Additionally, interaction between TS with SHMT (thymidylate biosynthesis cycle partner), CK2α (known to phosphorylate TS), and with unrelated protein, lipase Amano AY30, was investigated. The results obtained with SHMT, as well as with lipase Amano

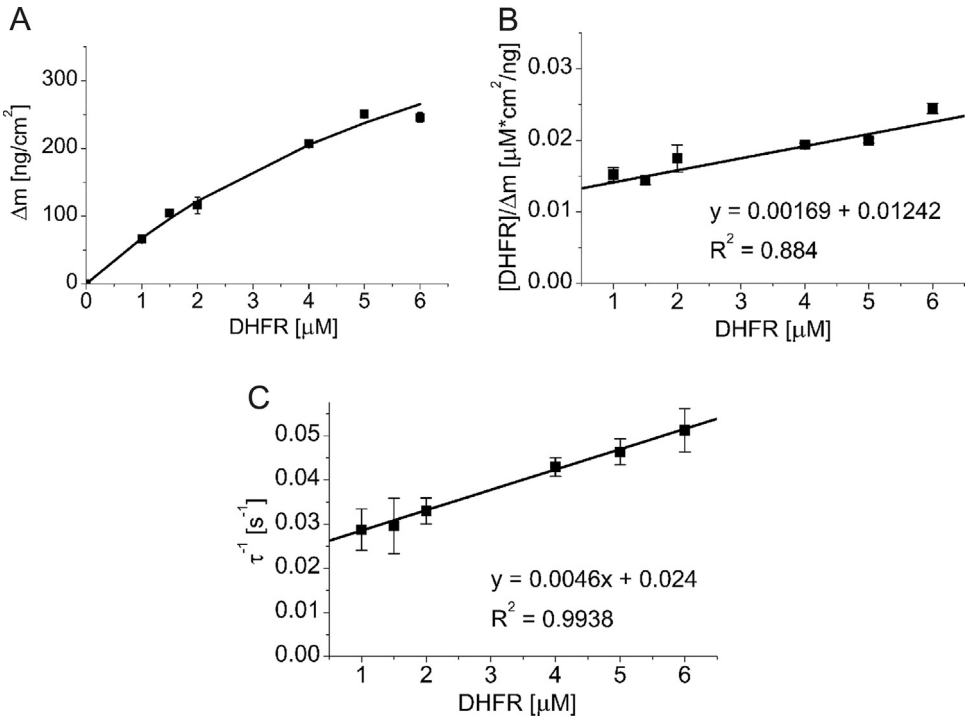

Fig. 1. QCM-D study of protein–protein binding kinetics. (A) Langmuir isotherm for 1–6 μM DHFR binding to the TS-modified sensor. (B) Linear regression of the Langmuir isotherm. (C) Linear dependence between relaxation rate constant and DHFR concentration (1–6 μM).

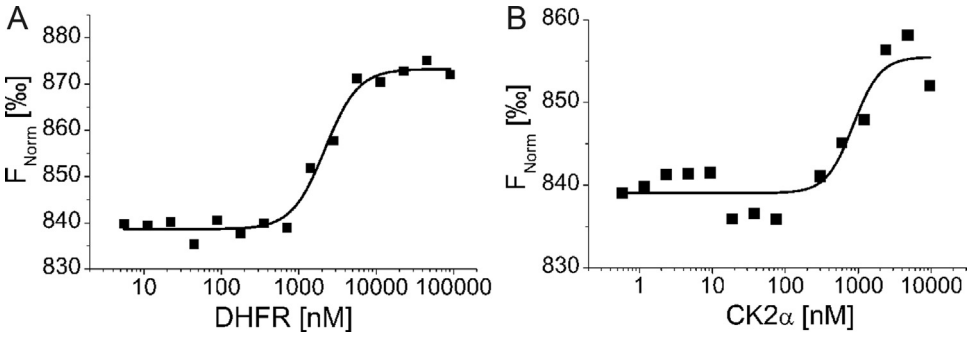

Fig. 2. Microscale thermophoresis study of protein–protein binding affinity. Direct study of interaction between fluorescently labeled TS and DHFR (A) or CK2α (B). The normalized thermophoresis signals were plotted against the DHFR or CK2α concentrations, respectively. TS concentration was kept constant at 0.3 μM, whereas DHFR was titrated from 5.54 nM to 181.5 μM and CK2α was titrated from 0.58 nM to 19.1 μM.

AY30 did not show a proper curve, pointing to lack of their interaction with TS. However, TS was able to form a strong complex with CK2α, a kinase which has earlier been shown to phosphorylate Ser124 residue on TS molecule (Frączyk et al., 2010). TS interacted with CK2α, forming a protein complex with K_d value of 1.08 ± 0.23 μM (two independent experiments). Dependence of F_{Norm} on CK2α concentration in the presence of labeled TS is given in Fig. 2B. Subsequent TS–CK2α kinetics parameters value was calculated as $K_a = 0.97 \pm 0.20\ \mu M^{-1}$ and $\Delta G = -34.1 \pm 0.5$ kJ/mol.

Binding characteristics for TS–DHFR complex formation were analyzed by Scatchard plot (Fig. 3B). Calculated stoichiometry points to binding ratio of 1 mol TS to 6.3 ± 0.4 mol DHFR. Obtained curvature for TS–DHFR indicates existence of multiple nonidentical binding sites on the TS dimeric protein displaying positive cooperativity upon interacting with binding partner. Since TS occurs in physiological state as a homodimer, this result may indicate that binding of DHFR to one subunit of TS dimer enhances affinity of the second TS subunit for DHFR.

Scatchard plot for TS–CK2α likewise denote the positive cooperation of multiple binding sites on the TS molecule. Interaction stoichiometry signalize the binding ratio of 1 mol TS to 1.9 ± 0.7 mol CK2α (not shown).

3.3. Comparison of QCM-D and MST results

The presented results show the formation of the complex between human enzymes involved in thymidylate synthesis, namely thymidylate synthase and dihydrofolate reductase. Two advanced techniques, quartz microbalance with dissipation monitoring and microscale thermophoresis, were utilized in the experiments allowing us to prove that human TS and DHFR proteins specifically interact with each other *in vitro*. Kinetic parameters of DHFR–TS complex formation obtained in QCM-D experiments are highly corresponding to data gained by means of MST. Determined dissociation constants (K_d) are in micromolar range value pointing to strong, specific interaction. Computed Gibbs free energy values of approximately -30 kJ/mol indicates the noncovalent interactions, suggesting the involvement of hydrogen and/or ionic bonds in the stabile protein complex. Moreover, Scatchard analysis of experimental data resulting from both methods suggests that 1 mol of TS binds approximately 6 mol of DHFR, which would mean three monomeric DHFR molecules per each TS subunit. Comparison of parameters obtained by both techniques is given in Table 1.

QCM-D analysis enabled us to gain the equilibrium dissociation constant *via* three methods: the Langmuir isotherm, relaxation rate constants and Scatchard plot. The values calculated from Langmuir isotherm and Scatchard equation are in a very good agreement (7.6 ± 0.7 and 7.5 ± 0.6 μM, respectively). The value calculated from the relaxation rate constants is slightly lower (5.1 ± 2.8 μM) but closer to the value obtained during MST measurements (2.8 ± 0.4 μM). This might be associated with the fact that one of the assumptions of Langmuir model is that the receptor active sites are independent – the probability of occupying one site is not dependent on the adjacent sites. Linear Scatchard plot in QCM-D experiment shows, that indeed there is no cooperativity between binding sites. However, MST results seem to point to the positive cooperativity in the complex formation. It is possible that in thermophoresis experiments, carried out in buffer solutions, both subunits of TS dimers are simultaneously equally available for DHFR proteins.

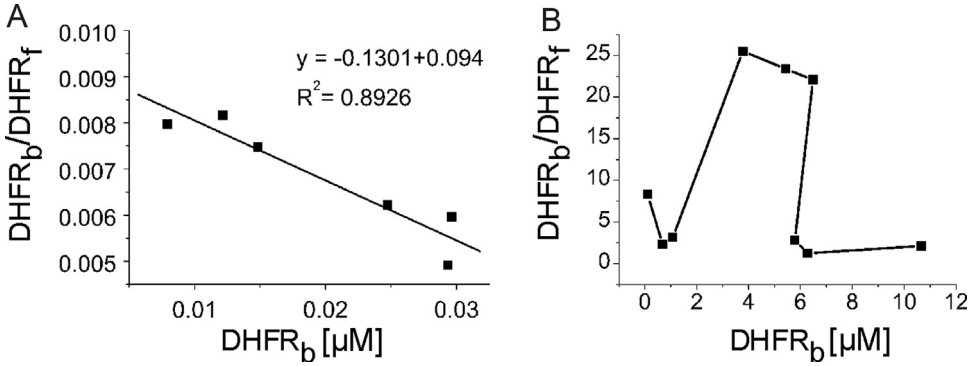

Fig. 3. Scatchard plots for TS–DHFR binding studied by means of (A) quartz crystal microbalance with dissipation monitoring and (B) microscale thermophoresis. Calculation of the concentrations of free and bound DHFR are given in Section 2.

Table 1
Comparison of kinetic parameters of TS–DHFR binding obtained *via* QCM-D and MST measurements.

	QCM-D	MST
$k_{on} \times 10^4$ (M^{-1} s^{-1})	0.46 ± 0.11	–
k_{off} (s^{-1})	0.024 ± 0.006	–
K_a (μM^{-1})	0.13 ± 0.01[a]	0.37 ± 0.06
	0.20 ± 0.12[b]	
K_d (μM)	7.6 ± 0.7[a]	2.8 ± 0.4
	5.1 ± 2.8[b]	
	7.5 ± 0.6[c]	
ΔG (kJ/mol)	-29.19 ± 0.21[a]	-31.7 ± 0.4
	-30.2 ± 1.3[b]	
DHFR/TS molar ratio[c]	6.19 ± 0.23	6.3 ± 0.4

[a] Parameters obtained *via* Langmuir isotherm.
[b] Parameters determined from the relaxation rate constant.
[c] Parameters determined from Scatchard plot.

Immobilization of TS protein on QCM-D sensor may conceal the cooperativity by subsequent saturation of TS subunits.

Using QCM-D we have also tried to characterize DHFR–TS complex kinetics by different approach, in which HisTag labeled DHFR was immobilized on the surface of the quartz crystal sensor and varying concentrations of HisTag free TS were introduced into the system. The obtained results showed no protein–protein interactions (Supporting information, Appendices B (Fig. B.5)). This might indicate that the residues near the N-terminus of DHFR may be involved in TS binding and therefore, blocked DHFR amino end prevents complex formation. The other possibility is that DHFR needs to change its conformation in order to fit the TS binding interface. Clearly, protein immobilization on a solid surface might prevent it from undergoing certain structural changes, as the conformational and rotational entropy is affected.

Furthermore, MST and QCM-D studies have proven that TS does not interact *in vitro* with SHMT, the third enzyme of the thymidylate biosynthesis cycle. Taking into account the results presented by Anderson et al. (2012), demonstrating the role of SHMT as an anchor of *de novo* thymidylate synthesis pathway to nucleus, it is plausible that TS and DHFR form an initial di-complex, which is subsequently linked and located by SHMT to nucleus.

DHFR and TS are highly important drug targets. DHFR inhibitors are used extensively in the therapy of leukemia, lymphoma and choriocarcinoma, while TS inhibitors are primary drugs in chemotherapy aimed at cancers of the gastrointestinal tract, head and neck (Phan et al., 2001). However, there emerges a problem in medical applications of DHFR and TS inhibitors due to the development of drug resistance. Understanding of the interactions between these two proteins may be useful in searching for new type of treatment. If TS–DHFR binding is a necessary step in DNA synthesis and repair, it is plausible to design drugs targeting the formation of the enzymatic complex. Designing of such drug types would be based on assumptions that TS–DHFR binding might either facilitate substrate transfer between the enzymes' active sites (*via* channeling, domain-domain interactions and cooperativity) or might be necessary for thymidylate synthase translocation to the nucleus (Anderson et al., 2012; MacFarlane et al., 2011; Woeller et al., 2007), or both.

4. Conclusions

We have proven the specific protein–protein complex formation between human thymidylate synthase and dihydrofolate reductase, two enzymes involved in thymidylate biosynthesis cycle. The quantification of determined interaction revealed strong binding of approximately 6 mol of DHFR to 1 mol of TS with dissociation constants in micromolar range. Gibbs free energy value for the complex pointed to hydrogen bonds and/or ionic interactions participating in complex formation. Moreover MST data revealed positive binding cooperativity between partner proteins, suggesting that the occupancy of one site of TS changes the affinity for DHFR of another TS site.

The demonstrated QCM-D and MST methods provide efficient means for characterizing protein–protein interactions. Both techniques allowed us to obtain compatible kinetic parameters, namely the equilibrium association and dissociation constants (K_a, K_d), association and dissociation rate constants (k_{on}, k_{off}), Gibbs free energy value (ΔG) and the stoichiometry of the complex. Coupling of the two methods allows for a credible *in vitro* insight into protein complex formation proving that QCM-D and MST might be used as potent complementary methods.

Acknowledgments

Studies have been supported by National Science Centre (Poland) Grant 2011/03/B/NZ1/00135, European Union within European Social Fund Human Capital and Warsaw University of Technology. We wish to thank NanoTemper Technologies (www.nanotemper-technologies.com) for providing the Monolith NT.115 instrument and their expert assistance. We also thank Dr. Monika Wielechowska for casein kinase CK2α samples used in these experiments.

Appendix. Supplementary information

Supplementary data associated with this article can be found in the online version at http://dx.doi.org/10.1016/j.bios.2014.08.031.

References

Anderson, D.D., Woeller, C.F., Chiang, E.-P., Shane, B., Stover, P.J., 2012. J. Biol. Chem. 287, 7051–7062.
Banerjee, D., Mayer-Kuckuk, P., Capiaux, G., Budak-Alpdogan, T., Gorlick, R., Bertino, J.R., 2002. Biochim. Biophys. Acta 1587, 164–173.
Carreras, C.W., Santi, D.V., 1995. Annu. Rev. Biochem. 64, 721–762.
Cooper, M., Singleton, V., 2007. J. Mol. Recognit. 20, 154–184.
Derler, I., Plenk, P., Fahrner, M., Muik, M., Jardin, I., Schindl, R., Gruber, H.J., Groschner, K., Romanin, C., 2013. J. Biol. Chem. 288, 29025–29034.
Duhr, S., Braun, D., 2006. Proc. Natl. Acad. Sci. USA 103, 19678–19682.
Ebara, Y., Okahata, Y., 1994. J. Am. Chem. Soc. 116, 11209–11212.
Frączyk, T., Kubiński, K., Masłyk, M., Cieśla, J., Hellman, U., Shugar, D., Rode, W., 2010. Bioorg. Chem. 38, 124–131.
Hook, F., Kasemo, B., 2001. Anal. Chem. 73, 5796–5804.
Hallström, T., Siegel, C., Mörgelin, M., Kraiczy, P., Skerka, C., Zipfel, P.F., 2013. mBio 4 (4), e00481.
Jerabek-Willemsen, M., Wienken, C.J., Braun, D., Baaske, P., Duhr, S., 2011. Assay Drug Dev. Technol. 9, 342–353.
Kisliuk, R., 2006. eLS.
Latz, A., Mehlmer, N., Zapf, S., Mueller, T.D., Wurzinger, B., Pfister, B., Csaszar, E., Hedrich, R., Teige, M., Becker, D., 2013. Mol. Plant 6 (4), 1274–1289.
Limson, J., Odunuga, O.O., Green, H., Hook, F., Blatch, G.L., 2004. S. Afr. J. Sci. 100, 678–682.
Liu, H., Thaker, Y.R., Stagg, L., Schneider, H., Ladbury, J.E., Rudd, C.E., 2013. J. Biol. Chem. 288, 29539–29549.
Liu, J., Schmitz, J.C., Lin, X., Tai, N., Yan, W., Farrell, M., Bailly, M., Chen, T., Chu, E., 2002. Biochim. Biophys. Acta 1587, 174–182.
MacFarlane, A.J., Anderson, D.D., Flodby, P., Allen, R.H., Stabler, S.P., Stover, P.J., 2011. J. Biol. Chem. 286, 44015–44022.
McGaughey, K.M., Wheeler, L.J., Moore, J.T., Maley, G.F., Maley, F., Mathews, C.K., 1996. J. Biol. Chem. 271, 23037–23042.
Melles, E., Anderson, H., Wallinder, D., Shafqat, J., Bergman, T., Aastrup, T., Jornvall, H., 2005. Anal. Biochem. 341 (1), 89–93.
Miles, L.A., Crespi, G.A.N., Doughty, L., Parker, M.W., 2013. Sci. Rep. 3, 1302.
Möller, M., Denicola, A., 2002. Biochem. Mol. Biol. Educ. 30, 309–312.
Nicolini, C., Bragazzi, N., Pechkova, E., 2012. Adv. Drug Deliv. Rev. 64, 1522–1531.
Okahata, Y., Niikura, K., Furusawa, H., Matsuno, H., 2000. Anal. Sci. 16, 1113–1119.

Pei, Z., Anderson, H., Aastrup, T., Ramstrom, O., 2005. Biosens. Bioelectron. 21, 60–66.
Phan, J., Koli, S., Minor, W., Dunlap, R.B., Berger, S.H., Lebioda, L., 2001. Biochemistry 40, 1897–1902.
Reddy, G.P., Pardee, A.B., 1980. Proc. Natl. Acad. Sci. USA 77, 3312–3316.
Sadik, O.A., Cheung, M.C., 2001. Talanta 55 (5), 929–941.
Seidel, S.A.I., Dijkman, P.M., Lea, W.A., Bogaart, G., Jerabek-Willemsen, M., Lazic, Joseph, J.S., Srinivasan, P., Baaske, P., Simeonov, A., Katritch, I., Melo, F.A., Ladbury, Schreiber, G., Watts, A., Braun, D., Duhr, S., 2013. Methods 59, 301–315.
Shen, D.Z., Huang, M.H., Chow, L.M., Yang, M.S., 2001. Sens. Actuators B 77 (3), 664–670.
Si, S.H., Si, L., Ren, F.L., Zhu, D.R., Fung, Y.S., 2002. J. Colloid Interface Sci. 253 (1), 47–52.
Spera, R., Festa, F., Bragazzi, N.L., Pechkova, E., LaBaer, J., Nicolini, C., 2013. J. Proteome Res. 12, 5535–5547.
Tan, L., Xie, Q., Jia, X., Guo, M., Zhang, Y., Tang, H., Yao, S., 2009. Biosens. Bioelectron. 24, 1603–1609.
Volpato, J.P., Pelletier, J.N., 2009. Drug Resist. Update 12, 28–41.
Voros, J., 2004. Biophys. J. 87 (1), 553–561.
Wienken, C.J., Baaske, P., Rothbauer, U., Braun, D., Duhr, S., 2010. Nat. Commun. 1, 100.
Wilson, P.M., Danenberg, P.V., Johnston, P.G., Lenz, H.-J., Ladner, R.D., 2014. Nat. Rev. Clin. Oncol. 11, 282–298.
Woeller, C.F., Anderson, D.D., Szebenyi, D.M., Stover, P.J., 2007. J. Biol. Chem. 282, 17623–17631.